Available online at www.sciencedirect.com
SCIENCE DIRECT®
European Journal of Medicinal Chemistry 40 (2005) 1103–1110
EUROPEAN JOURNAL OF MEDICINAL CHEMISTRY
www.elsevier.com/locate/ejmech

Original article

Synthesis, antibacterial, antifungal activity and interaction of CT-DNA with a new benzimidazole derived Cu(II) complex

Farukh Arjmand [a,*], Bhawana Mohani, Shamim Ahmad [b]

[a] *Department of Chemistry, Aligarh Muslim University, Aligarh, UP, India*
[b] *Institute of Ophthalmology, J.N. Medical College, Aligarh Muslim University, Aligarh, UP, India*

Received 29 December 2004; received in revised form 13 May 2005; accepted 18 May 2005

Available online 11 July 2005

Abstract

The ligand $[C_{16}H_{10}O_2N_4S_2]$ **L** has been synthesized by the condensation reaction of 2-mercaptobenzimidazole and diethyloxalate. The ligand **L** was allowed to react with bis(ethylenediamine)Cu^{II}/Ni^{II} complexes to yield $[C_{20}H_{22}N_8S_2Cu]Cl_2$ **1** and $[C_{20}H_{22}N_8S_2Ni]Cl_2$ **2** complexes. The Ni(II) complex was synthesized only to elucidate the structure of the complex. The complexes **1** and **2** were characterized by elemental analyses, IR, NMR, EPR, UV–vis spectroscopy and molar conductance measurements. Both the complexes are ionic in nature and possess square–planar geometry. The binding of the complex **1** to calf thymus DNA was investigated spectrophotometrically. The absorption spectra of complex **1** exhibits a slight red shift with "hyperchromic effect" in presence of CTDNA. Electrochemical analysis and viscosity measurements were also carried out to ascertain the mode of binding. The complex **1** in the absence and in presence of CT DNA in aqueous solution exhibits one quasi-reversible redox wave corresponding to Cu^{II}/Cu^{I} redox couple at a scan rate of 0.2 V s^{-1}. The shift in ΔE_p, $E_{1/2}$ and I_{pa}/I_{pc} values ascertain the interaction of calf thymus DNA with copper(II) complex. There is decrease in viscosity of CTDNA which indicates that the complex **1** binds to CTDNA through a partial intercalative mode. The antibacterial and antifungal studies of the $[C_7H_6N_2S]$, $[C_4H_{16}N_4Cu]Cl_2$, $[C_{16}H_{10}N_4S_2O_2]$ and $[C_{20}H_{22}N_8S_2Cu]Cl_2$ were carried out against *S. aureus*, *E. coli* and *A. niger*. All the results reveal that the complex **1** is highly active against the bacterial strains and also inhibits fungal growth.

Keywords: Mercaptobenzimidazole; Cu(II) complex; CTDNA interaction; Spectrophotometry; Cyclic voltammetry; Viscosity; Antibacterial and antifungal activity

1. Introduction

There is a considerable interest in the pharmacology of heterocyclic ligands and their metal chelates [1,2]. In general, nitrogen and sulfur containing organic compounds and their metal complexes display a wide range of biological activity [3–6], as antitumor, antibacterial, antifungal and antiviral agents. Benzimidazole substituted derivatives are inhibitors of cyclin-dependent kinase and useful for inhibiting cell proliferation, in for the treatment of cancer. The activity of these compounds have been determined by cyclin-dependent kinase (CDK) 4/cyclin D1 and CDK2/cyclin E flashplate assays [7].

Bis-benzimidazoles have potent activity against a number of microorganisms including those that lead to AIDS-related infections [8]. These compounds bind to DNA in AT-rich sequences [9] Recently, benzimidazole derived drugs have received much attention owing to the fact that benzimidazole residue is a constituent of vitamin B_{12} [9] which supports their potential use as therapeutics [10]. Benzimidazole, sometimes called 1,3-dideazapurine and its derivatives can serve as model compounds for purine due to the structural similarity [11,12].

Copper complexes have been extensively utilized in metal-mediated DNA cleavage for the generation of activated oxygen species [13,14]. It has been reported that tetraaza macrocyclic copper complexes have shows anti-HIV activities, furthermore copper accumulates in tumors due to the selective permeability of cancer cell membranes to copper compounds. For this reason, a number of copper complexes were screened for anticancer activity and some of them were found active both in vivo and in vitro [15,16].

* Corresponding author.
E-mail addresses: farukh_arjmand@yahoo.co.in (F. Arjmand), shamim@rediffmail.com (S. Ahmad).

0223-5234/$ - see front matter © 2005 Elsevier SAS. All rights reserved.
doi:10.1016/j.ejmech.2005.05.005

To design improved drugs that target the cellular DNA and to understand the mechanism of action at the molecular level, we have synthesized new benzimidazole ligand $[C_{16}H_{10}O_2N_4S_2]$ and its metal complexes $[C_{20}H_{22}N_8S_2Cu]\cdot Cl_2$ and $[C_{20}H_{22}N_8S_2Ni]\cdot Cl_2$. Binding studies of the potential drug complex $[C_{20}H_{22}N_8S_2Cu]\cdot Cl_2$ with calf thymus DNA (CTDNA) were studied by electronic absorption spectroscopy, cyclic voltammetric and viscosity measurements. Antibacterial and antifungal activities of the complex $[C_{20}H_{22}N_8S_2Cu]Cl_2$ were screened against *S. aureus* and *E. coli* (bacteria) and *A. niger* (fungus).

2. Experimental

2.1. Reagents

2-Mercaptobenzimidazole (Fluka), diethyl oxalate, $NiCl_2\cdot 6H_2O$ and $CuCl_2\cdot 2H_2O$ ethylenediamine (Merck) were used as received.

2.2. Other physical measurements

Microanalyses of the complexes were obtained on a Carlo Erba Analyzer Model 1106. Molar conductances were measured at room temperature on a Digisun Electronic Conductivity Bridge. IR spectra (200–4000 cm^{-1}) were recorded on a Carl Ziess specord M-80 spectrophotometer in Nujol mull. ^1H and ^{13}C NMR spectra were recorded on an amx-500 spectrometer. The EPR spectra were obtained on a Varian E112 spectrometer at X-band frequency (9.1 GHz) at liquid nitrogen temperature (LNT).

Cyclic voltammetry was carried out at CH instrument electrochemical analyzer. High purity H_2O and DMSO (95:5) was employed for the cyclic voltammetric studies with 0.4 M KNO_3 as a supporting electrolyte. A three electrode configuration was used comprising of a Pt disk working electrode, Pt wire counter electrode and Ag/AgCl as reference electrode. The kinetic experiments were performed under pseudo-first order conditions and the spectral changes were recorded at 628 nm (λ_{max} of complex **1** + CTDNA) with respect to time using a (USB2000) Ocean Optics spectrophotometer. Viscosity measurements were carried out using Ostwald's viscometer at 29 ± 0.01 °C. Flow time was measured with a digital stop-watch. Each sample was measured three times and an average flow time was calculated. Data were presented as (η/η_0) versus binding ratio ([Cu]/[DNA]) [17], where η is a viscosity of DNA in the presence of complex and η_0 is the viscosity of DNA alone. Viscosity values were calculated from the observed flow time of DNA containing solution ($t > 100$ s) corrected for the flow time of buffer alone (t_0), $\eta = t - t_0$.

2.3. Antibacterial screening

The antibacterial activity of $[C_7H_6N_2S]$, $[C_{12}H_{16}N_4Cu]Cl_2$, $[C_{16}H_{10}N_4S_2O_2]$ and $[C_{20}H_{22}N_8S_2Cu]Cl_2$ were screened against *E. coli* and *S. aureus* in DMSO by the well diffusion method using standard Mueller–Hinton agar as the medium [18].

Sensitivity plates were inoculated with *E. coli* and *S. aureus* and the well was loaded with (140 μl) of test compound solution using a micropipette. The incubation was done for 24 h at 37 °C. During this period, the test solution diffused zones of inhibition which were recorded using Vernier callipers. The radius of the zone is the measure of antibacterial activity.

To evaluate the effect of concentration on antibacterial activity, four different concentrations (10, 20, 30 and 40 μg ml^{-1}) of the test compounds were screened against *E. coli* and *S. aureus* in DMSO by employing the same procedure.

2.4. Antifungal screening

Antifungal activity of the $[C_7H_6N_2S]$, $[C_4H_{16}N_4Cu]Cl_2$, $[C_{16}H_{10}N_4S_2O_2]$ and $[C_{20}H_{22}N_8S_2Cu]Cl_2$ evaluated using the Sabouroud dextrose agar diffusion method. Wells were made (8 mm diameter) with a sterile cork borer. To these wells 140 μl from each (10, 20, 30 and 40 μg ml^{-1}) of the test stock solution compounds were added and the plates were allowed to cool for an hour to facilitate the diffusion. The plates were then incubated at 37 °C for 48 h. At the end of the incubation period, the diameter of the zone of inhibition around the wells was measured.

2.5. Synthesis of ligand $[C_{16}H_{10}O_2N_4S_2]$ L

2-Mercaptobenzimidazole (5 g, 0.033 mol) was dissolved in MeOH (100 ml) and to this solution was added diethyl oxalate (2.26 g, 0.016 mol) in a 2:1 molar ratio. The solution was refluxed for ca. 1 h, then conc. HCl (6 ml) was added dropwise with constant stirring. The cream crystalline product which formed was filtered off under vacuum, washed thoroughly with hexane and dried in vacuo. Yield 74% m.p. 100 ± 1 °C (Found: C, 54.26; H, 2.81; N, 15.83. $C_{16}H_{10}O_2N_4S_2$%) requires C, 54.23; H, 2.82; N, 15.81. IR/cm^{-1} (Nujol mull): 1688 ν(C=O), 2472 ν(SH), 1304 ν(C–N). δ_H (300 MHz, D_2O, TMS) 7.73–7.85 (ArH), 3.8 (SH). δ_c 128 (ArC), 165 (C=O).

2.6. Synthesis of $[C_4H_{16}N_4Cu]Cl_2$ and $[C_4H_{16}N_4Ni]Cl_2$

These compounds were synthesized by the method reported earlier [19].

2.7. Synthesis of the $[C_{20}H_{22}S_2N_8Cu]\cdot Cl_2$

To a solution of the ligand (1 g, 0.003 mol) in MeOH (50 ml) was added $[Cu(en)_2]\cdot Cl_2$ (0.76 g 0.003 mol) in the same solvent. The resulting mixture was magnetically stirred for ca. 2 h. The blue precipitate formed was isolated, washed with hexane and dried in vacuo (Scheme 1). Yield 62% m.p. 250 ± 2 °C (Found: C, 41.94; H, 3.85; N, 19.53.

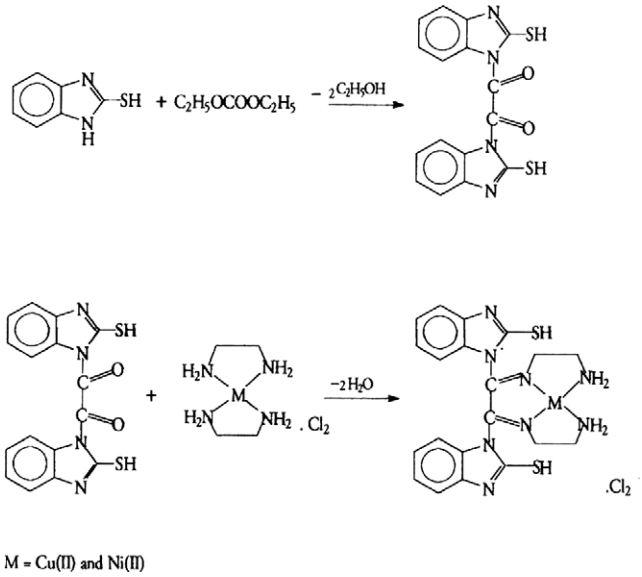

Scheme 1.

$[C_{20}H_{22}S_2N_8Cu]\cdot Cl_2$%) requires C, 41.91; H, 3.84; N, 19.56. IR/cm^{-1} (Nujol mull): 2476 υ(SH), 1306 υ(C–N), 2942, 1508, 677 $\upsilon(CH_2)$, 3357 $\upsilon(NH_2)$, 1639 υ(C=N) 425 υ(M–N).

2.8. Synthesis of the $[C_{20}H_{22}S_2N_8Ni]\cdot Cl_2$

A similar procedure was also adopted for the Ni^{II} complex. Yield 56% m.p. 263 ± 2 °C (Found: C, 42.3; H, 3.8; N, 19.7. $[C_{20}H_{22}S_2N_8Ni]\cdot Cl_2$ requires C, 42.27; H, 3.87; N, 19.72%). IR/cm^{-1} (Nujol mull): 2475 υ(SH), 1303 υ(C–N), 2940, 1509, 675 $\upsilon(CH_2)$, 3359 $\upsilon(NH_2)$, 1645 υ(N=C), 445 υ(M–N). δ_H (300 MHz, DMSO-d_6, TMS) 7.72–7.84 (ArH), 3.8 (SH), 5.2 (NH_2), 3.70–3.84 (CH_2). δ_c 128.8 (ArC), 170 (>C=N), 49.20 (CH_2), 117.2 (>C–N).

3. Result and discussion

3.1. IR spectra

The ligand L shows a medium intensity band at 2474 cm^{-1} assigned to –SH group, which remains unaltered suggesting the noninvolvement of this group in coordination with diethyl oxalate [20]. The characteristic bands at 3100 and 1490 cm^{-1} due to υ(NH) stretching and bending vibration [21], respectively, were not observed in IR spectrum of ligand indicating the ligand formation take place through –NH group of imidazole ring.

In the complexes, the characteristic band at ca. 1688 cm^{-1} attributed to υ(C=O) disappears [22], with the emergence of a new strong band at 1639–1645 cm^{-1} region which indicates the condensation of υ(C=O) group with NH_2 group of bis-(ethylenediamine) Cu^{II}/Ni^{II} complexes. The formation of υ(C=N) band, and the disappearance of the υ(C=O) band in the complexes commensurate with effective Schiff's base condensation [23]. The alkyl CH_2 group shows characteristic stretching absorption bands in the region 2942, deformation band at 1508 and rocking modes at 677 cm^{-1}, respectively [24]. A medium intensity band at 3357 cm^{-1} was observed in the complexes which was assigned to $\upsilon(NH_2)$ groups of the other side of bis(ethylenediamine) moiety suggesting1:1 condensation reaction [25]. In the IR region, the bands appearing at 425 and 445 cm^{-1} have been assigned to υ(Cu–N) and υ(Ni–N), which further confirm the formation of the complexes [26].

3.2. Electronic spectra

The electronic spectrum of the complex **1** in DMSO reveals a broad band at ca. 15,2207 cm^{-1} assignable to $^2B_{1g} \rightarrow {}^2A_{1g}$ transition [27,28] which is characteristic of square planar environment around the copper(II) ion. The complex **2** displays two bands at ca. 17,000 and 24,075 cm^{-1} regions which are assigned to $^1A_1(F) \rightarrow {}^1B_1(G)$ and $^1A_{1g} \rightarrow {}^1A_{2g}$ transitions, respectively, characteristic of typical square–planar geometry [29]. A strong charge transfer (LMCT) bands at ca. 35,673 and 30,000 cm^{-1} region appear in all the complexes attributed to the π–π^* transition.

3.3. NMR spectra

In order to elucidate the structural features of the compounds, ^1H and ^{13}C NMR spectra of the ligand **L** and the complex **2**, recorded in D_2O and DMSO, respectively, were examined. The ^1H NMR spectrum of ligand, exhibits a intense signals at 3.8 ppm which were assigned to –SH protons [30]. The absence of band at ca. 12 ppm due to NH protons suggest deprotonation of –NH group of the imidazole ring. In addition, the spectrum of the ligand exhibits multiplet at 7.73–7.85 ppm, which shows the presence of phenyl protons [31]. The ^{13}C NMR spectrum of the ligand exhibits signals at 165.70 and 128.0 ppm assigned to > C=O group and phenyl carbons, respectively.

The ^1H NMR spectrum of the complex **2** displays signals at 5.2 and 3.7–3.84 ppm due to $–NH_2$ and $–CH_2$ protons, respectively [32,33]. These signals further support the formation of complex by 1:1 condensation reaction. The ^{13}C NMR spectrum of the complex strongly supports the Schiff base formation as signal at 165.70 assigned to > C=O disappears and two new signals were observed at 170 and 49.2 ppm attributed to > C=N and $–NCH_2$ carbons, respectively.

3.4. EPR spectra

The X-Band (≈9.1 GHz) EPR spectrum of the complex **1**was recorded at liquid nitrogen temperature (77 K) using tetracynoethylene (TCNE), as field marker. The $g_{\|}$, $g_{\perp}$ and g_{av} values computed from the spectrum were found to be 2.22, 2.07 and 2.11, respectively. The mathematical expression for g_{av} value is $g_{av}^2 = (g_{\|}^2 + 2g_{\perp}^2)/3$. The existence of $g_{11} > g_1$ suggest that $dx^2 - y^2$ is the ground state with the d^9 $[Cu^{2+}]$ configuration i.e. $(eg)^4$, $(a_{1g})^2$ $(b_{2g})^2$ $(b_{1g})^1$, which evidences

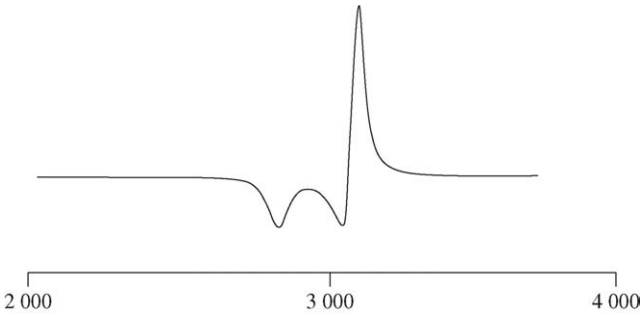

Fig. 1. X-band EPR spectrum of the Cu(II)complex at LNT.

the square planar environment around the copper(II) ion in the complex [34] (Fig. 1).

4. Electrochemistry

The cyclic voltammetry of the complex **1** was recorded in DMSO/H_2O (5:95) at room temperature at a scan rate of 0.2 V s^{-1} in the potential range 1.0 to –0.8 V (Fig. 2). The cyclic voltammogram of the complex **1** in absence of CTDNA exhibits a quasireversible redox wave for one electron transfer process corresponding to Cu^{II}/Cu^{I} redox couple with $E_{1/2}$ = 0.27 V and ΔE_p value of 288 mV. The ratio of the anodic and cathodic peak currents I_{pa}/I_{pc} is 1.33 implying quasireversible electron transfer. At different scan rates, the voltammogram does not show any major change. However, at various scan rates the peak height increases indicating the reversibility of the process (Fig. 3).

On addition of calf thymus DNA, complex **1** registers a significant shift in ΔE_p value as well as in $E_{1/2}$ values 105 and 17 mV, respectively, at the scan rate of 0.2 V s^{-1} (Fig. 4). The

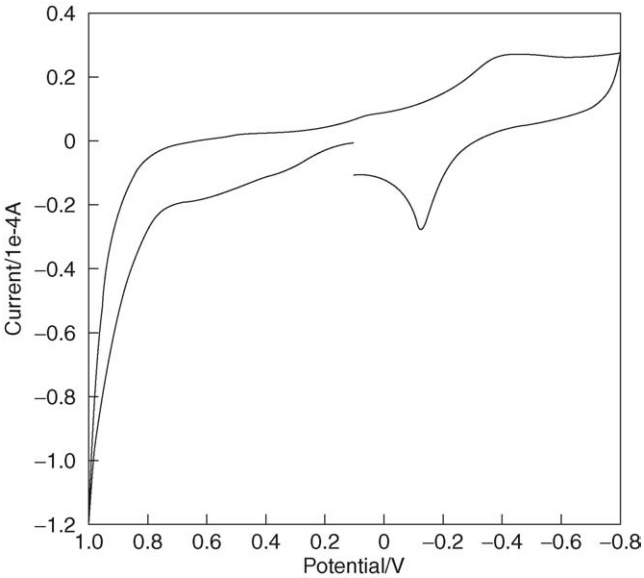

Fig. 2. Cyclic voltammogram of complex **1** in DMSO/H_2O (5:95) at 30 °C at a scan rate of 0.2 V s^{-1}.

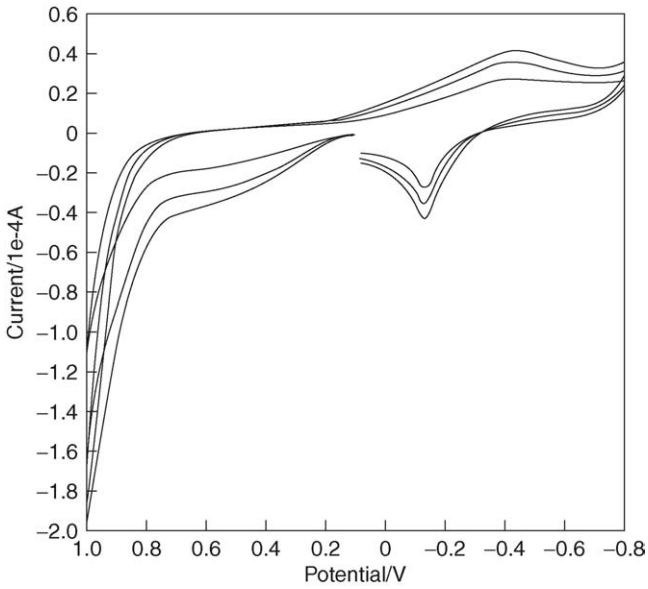

Fig. 3. Cyclic voltammograms of complex **1** in DMSO/H_2O (5:95) at 30 °C at different scan rates viz. 0.2, 0.3 and 0.4 V s^{-1}.

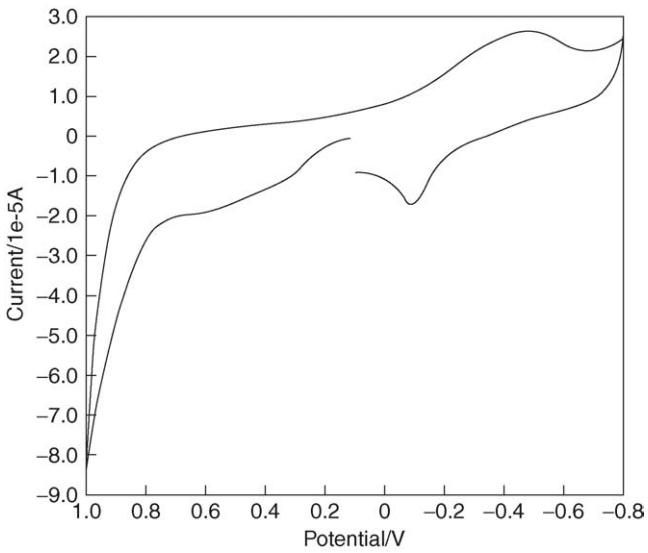

Fig. 4. Cyclic voltammogram of complex **1** in the presence of CTDNA at 30 °C at a scan rate of 0.2 V s^{-1}.

ratio of I_{pa}/I_{pc} = 0.67 for the calf thymus bound complex. The decrease in current is due to diffusion of an equilibrium mixture of free and DNA-bound metal complex to the electrode surface [35].

To elucidate the binding mechanism involving the Cu(II) or Cu(I) forms of complex to CTDNA, the net shift in $E_{1/2}$ can be used to estimate the ratio of equilibrium constants by the following equation.

$$E^{1/2} - E^{1/2'} = 0.0591 \log (K_{1+}/K_{2+})$$

The ratio of binding constants of +1 and +2 species was (0.9) close to 1, suggesting that both Cu(II) and Cu(I) forms interact with CTDNA to the same extent.

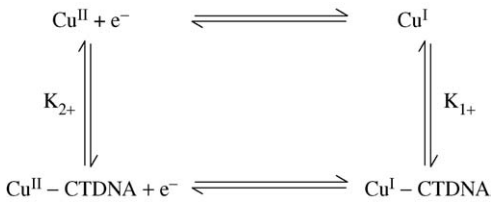

5. Kinetics studies

The absorption spectrum of the complex **1** (in absence of CTDNA) in DMSO reveals one intense well resolved MLCT band at 282 nm attributed to Cu(II) → π* of the benzimidazole ring and a broad band in the visible region at 657 nm assigned to d–d transition on addition of CTDNA to the complex **1** in Tris–HCl buffer/DMSO there is an increase in the absorbance (hyperchromism) in both CT band and the d–d band in the visible region and it is accompanied by a slight red shit. A similar hyperchromism was observed also for a Cu(II) complex with a ligand bearing NH and OH groups [36] and for the soret bands of certain porphyrins showing interactions with DNA [37]. "Hyperchromic effect" and "hypochromic effect" are spectral features of changes in DNA concerning its double-helix structure.

Kinetics of the interaction of complex **1** with CTDNA was carried out and is displayed in Figs. 5a,b. A kinetic absorption-trace was followed spectrophotometrically at 628 nm which is λ_{max} of complex **1** + CTDNA under pseudo first order conditions. The rate constant, k_{obs}, were obtained by the linear least squares regression method (Fig. 6).

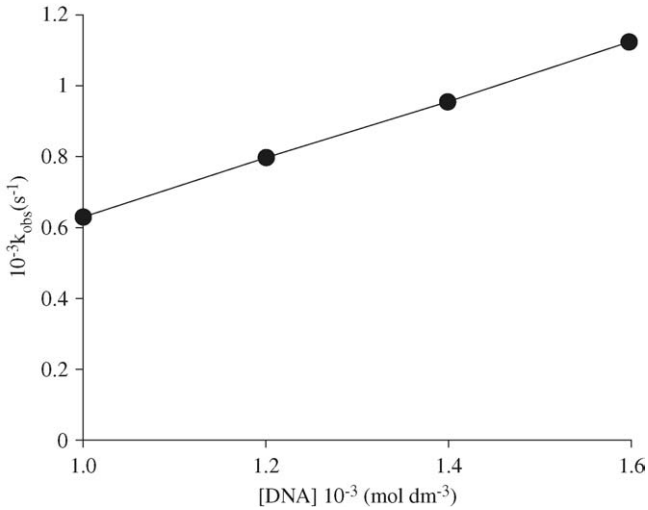

Fig. 6. Plot of $k_{obs,}$ versus DNA at varying concentration of CTDNA (1.0–1.6 × 10^{-5} mol dm^{-3}) and fixed concentration of the complex **1** = 0.1 × 10^{-5} mol dm^{-3}).

The concentration of complex **1** (0.1 × 10^{-3} M) was kept constant and concentration of CTDNA (1–1.6 × 10^{-3} M) was varied and the spectral changes were monitored with respect to time with increasing concentration of CTDNA, the absorption bands shows hyperchromism and a slight red shift in $\lambda_{max.}$ Although a slight red shift would be expected due to interaction between aromatic chromophores and DNA base pairs due to classical intercalative binding mode [38] but the

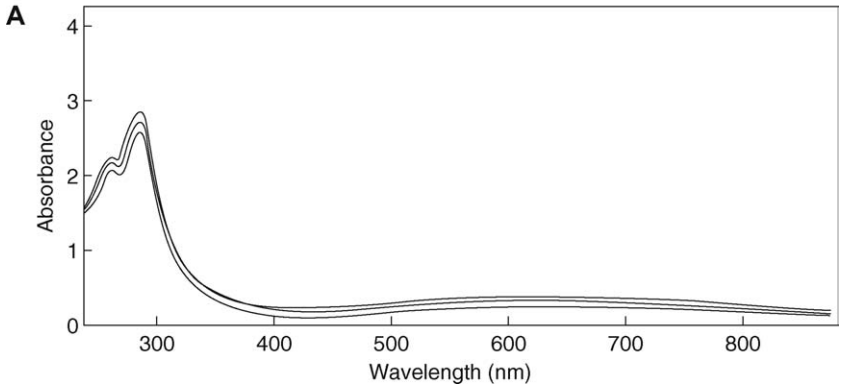

Fig. 5a. UV–vis spectrum of complex **1** (1 × 10^{-3} mol dm^{-3}) with increasing concentration of CTDNA (1–1.6 × 10^{-3} mol dm^{-3}) in Tris–HCl buffer solution.

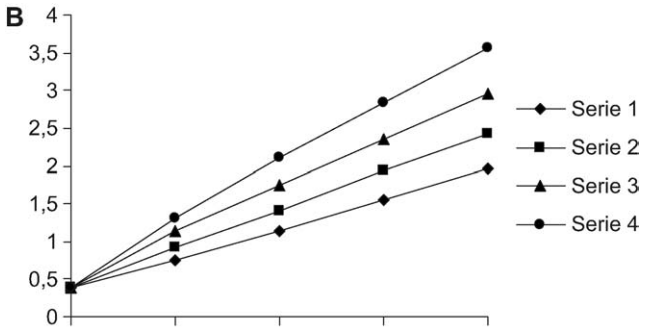

Fig. 5b. Plots of logA versus time for complex **1** at varying concentration of CTDNA (1–1.6 × 10^{-3} mol dm^{-3}).

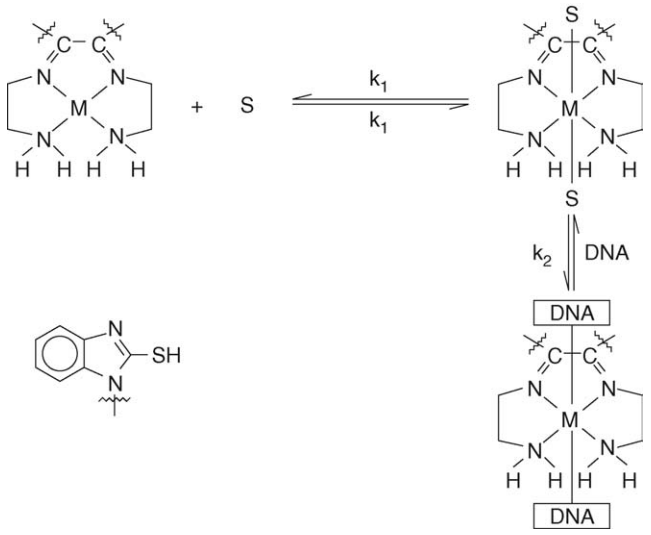

Scheme 2.

increase in intensity "hyperchromism" which may be attributed to total damage caused to DNA helix [39] which could not be a possible result of intercalation. Literature survey on benzimidazole derivatives reveal the binding with walls of DNA minor groove which are also supported by electrostatic, van der Waals and H-bonding interactions [40].

On the basis of kinetic data, the following mechanism, is proposed (Scheme 2).

The rate law has been derived

$$k_{obs} = k_1 k_2 [DNA]/[k_{-1} + k_2] \quad (1)$$

If the above rate law holds good, the proposed mechanism (Scheme 2) is correct. The plot of $k_{obs,}$ versus [DNA] gave a straight line with slope = $k_1 k_2 [k_{-1} + k_2]$ which is consistent with the proposed mechanism.

6. Viscosity measurements

To further clarify the nature of the interaction between the complex and DNA, viscosity measurements were carried out and the results are presented in Fig. 7. The experiment involves the measurement of the flow rate of DNA solution through a capillary viscometer. Hydrodynamic measurement that are sensitive to length change (i.e. viscosity and sedimentation) are regarded as the least ambiguous and most critical tests of a binding model in solution in the absence of crystallographic structural data [41,42]. The complex **1** proved to be very interesting species as it decreases the viscosity of the calf thymus DNA by varying concentration of added complex, signifying that Cu(II) complex binds to DNA through not by classical intercalation but by a partial intercalation mode [43]. Partial intercalation may act as a wedge to try apart one of a base-pair stack, but not fully separate the stack as required by the classical intercalation mode.

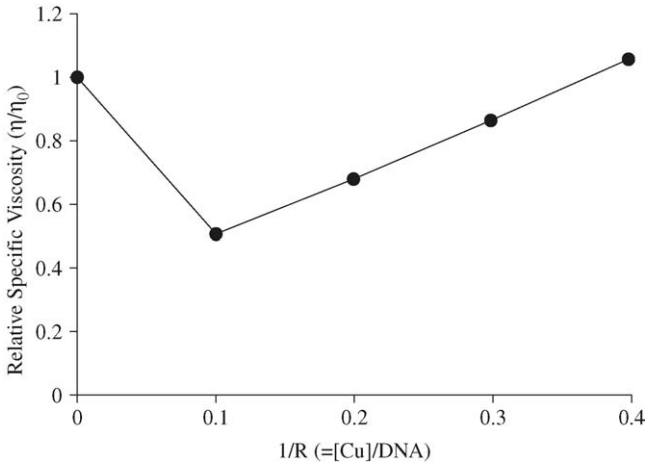

Fig. 7. Effect of increasing amount of complex **1** on the relative viscosity CTDNA at 25 ± 0.1 °C. [DNA] = 5×10^{-4}.

6.1. Antibacterial activity

Among the compounds tested, the complex **1** was found to be the most active against *S. aureus* and *E. coli* (Table 1). The order of inhibition was found to be:

Mercaptobenzimidazole < $[C_{16}H_{10}O_2N_4S_2]$ < $[Cu(en)_2]\cdot Cl_2$ < $[C_{20}H_{22}N_8S_2N_8Cu]Cl_2$.

6.2. Antifungal activity

The results of antifungal studies are presented in Table 2. The results shows that the complex **1** is more active in comparison to the other compounds against the *A. niger* under the identical experimental conditions. The increase in antifungal activity of the complex **1** can be ascribed to the effect of the metal ion on the normal cell process. The toxicity increase in the light of chelation theory [44] as chelation con-

Table 1
Antibacterial activity of the compounds with different concentrations (diameter of inhibition in mm)

Compound	Growth inhibition concentration Of the title compounds [complex] × 10^{-5} M	*S. aureus*	*E. coli*
$[C_{20}H_{22}N_8S_2Cu]Cl_2$ 1	1.7	19	17
	13	23	19
	20	25	22
	26	28	26
$[C_4H_{16}N_4Cu]Cl_2$	3.9	13	12
	7.8	15	14
	11.7	16	16
	15.6	13	17
$[C_{16}H_{10}N_4S_2O_2]$	2.8	11	11
	5.6	12	12
	8.4	14	14
	11.2	16	20
$[C_7H_6N_2S]$	6.6	11	12
	13.0	11	11
	20.0	13	12
	26.0	13	12

* Well diameter = 8 mm.

Table 2
Antifungal activity of the compounds with different concentrations (diameter of inhibition in mm)

Compound	Growth inhibition concentration of the title compounds [complex] × 10^{-5} M	*A. niger*
$[C_{20}H_{22}N_8S_2Cu]Cl_2$	1.7	19
	3.4	23
	5.1	25
	6.8	27
$[C_4H_{16}N_4Cu]Cl_2$	3.9	13
	7.8	15
	11.7	16
	15.6	18
$[C_{16}H_{10}N_4S_2O_2]$	2.8	11
	5.6	12
	8.4	14
	11.2	15
$[C_7H_6N_2S]$	6.6	9
	13	9
	20	9
	26	10

* Well diameter = 8 mm.

siderably reduces the polarity of the metal ion mainly because of partial sharing of its positive charge with donor groups and possible π-delocalization over the chelation ring. Such chelation could enhance the lipophilic character of the central metal atom, which subsequently favors its permeation through the lipid layer of the cell membrane. The presence of lipophilic and polar substituents such as C=N, S–H and NH_2 are expected to enhance the fungal toxicity and therefore copper(II) complex have a greater chance of interaction with the nucleotide bases.

Acknowledgments

Thanks to RSIC, CDRI Lucknow for providing C,H,N analysis data, NMR, and IIT Bombay for EPR measurements. The authors gratefully acknowledge Dr. Sartaj Tabassum, AMU, Aligarh for providing cyclic voltammetry facility.

References

[1] L. Mishra, A.K. Yadaw, J. Indian, Chem. 39A (2000) 660–663.
[2] A.D. Naik, S.M. Annigeri, U.B. Gangadharmath, V.K. Revankar, V.B. Mahale, Indian J. Chem. 24A (2002) 2046–2053.
[3] A.S. Pedrares, J. Romero, J.A.G. Vazquez, M.L. Duran, I. Casanova, A. Sousa, Dalton Trans. 7 (2003) 1379–1388.
[4] A.A. El-Asmy, M.E. Khalifa, M.M. Hassanian, J. Indian, Chem. 43A (2004) 92–97.
[5] J.K. Ekegren, P. Roth, K. Kallstrom, T. Tarnai, P.G. Andersson, Org. Biomol. Chem. 1 (2003) 358–363.
[6] F. Mevellec, F. Tisato, F. Refosco, A. Roucoux, N. Noiret, H. Patin, G. Bandoli, Inorg. Chem. 41 (2002) 598–601.
[7] F. Clerc, F. Hamy, I. Depaty, O.A. Boniface, S. Deprets, C. Carrez, M. Roesner, Curr. Opin. Investig. Drugs 4 (2003) 800.
[8] C.A. Bell, C.C. Dykstra, N.A. Naimen, M. Cory, T.A. Fairley, R.R. Tidwell, Antimicrob. Agents Chemother. 37 (1993) 2668–2673.
[9] D.J. Skalitzky, J.T. Marakovits, K.A. Maegley, A. Ekker, X.-H. Yu, Z. Hostomsky, S.E. Webber, B.W. Eastman, R. Almassy, J. Li, N.J. Curtin, D.R. Newell, A.H. Calvert, R.J. Griffin, B.T. Golding, J. Med. Chem. 46 (2003) 210–213.
[10] J.P. Lalezari, J.A. Aberg, L.H. Wang, M.B. Wire, R. Miner, W. Snowden, C.L. Talarico, S. Shaw, M.A. Jacobson, W.L. Drew, Antimicrob. Agents Chemother, 46 (2002) 2969–2976; N.H. Hauel, H. Nar, H. Prirpke, U. Ries, J.-M. Stassen, W. Wienen, J. Med. Chem. 45 (2002) 1757–1766; J. Valdez, R. Cedillo, A.H. Camos, L. Yepez, F.H. Luis, G.N. Vazquez, A. Tapia, R. Cortes, M. Hernandez, R. Castillo, Bioorg. Med. Chem. Lett. 12 (2002) 2221–2224.
[11] F. Seela, T. Wenzel, Helv. Chim. Acta 78 (1995) 833–846.
[12] M.J.S. Moreno, A.F. Botello, R.B.G. Coca, R. Griesser, J. Ochocki, A. Kotynski, J.N. Gutierrez, V. Moreno, H. Sigel, Inorg. Chem. 43 (2004) 1311–1322.
[13] J. Liu, H. Zhang, C. Chen, H. Deng, T. Lu, L. Ji, Dalton Trans. 1 (2003) 114–119.
[14] R. Nagane, M. Chikira, M. Oumi, H. Shindo, W.E. Antholine, J. Inorg. Biochem. 78 (2000) 243–249.
[15] N.K. Singh, S.B. Singh, Metal Based Drugs 9 (2002) 109–118.
[16] D. Jayaraju, A.K. Kondapi, Curr. Sci. 81 (2001) 787–792.
[17] G. Cohen, H. Eisenberg, Biopolymers 8 (1969) 45–55.
[18] R.S. Verma, W.L. Nobles, J. Pharm. Sci. 64 (1975) 881–887.
[19] G. Wilkinson, R.D. Gillard, J.A. McCleverty, "Comprehensive Coordination Chemistry", Perganon Press, Oxford, 1987 (2).
[20] B.S. Hammes, C.J. Carrano, J. Chem. Soc., Dalton Trans. 19 (2000) 3304–3309.
[21] B. Mohani, F. Arjmand, S. Tabassum, Transition Met. Chem. 27 (2002) 776–781.
[22] A.A. Tak, F. Arjmand, S. Tabassum, Transition Met. Chem. 27 (2002) 741–747.
[23] J. Zhang, P. Braunstein, R. Welter, Inorg. Chem. 43 (2004) 4172–4177.
[24] R.M. Silverstein, "Spectrometric Identification of Organic Compounds", Wiley, New York, 1974.
[25] A.S. El-Tabl, T.I. Kashar, R.M. El-Bahnasawy, A.E. Ibrahim, Pol. J. Chem. 73 (1999) 242–248.
[26] N. Raman, A. Kulandaisamy, K. Jeyasubramanian, J. Indian, Chem. 41A (2002) 942–949.
[27] M. Yonemura, K. Arimura, K. Inoue, N. Usuki, M. Ohba, H. Okawa, Inorg. Chem. 41 (2002) 582–589.
[28] K.K. Nanda, A.W. Addison, N. Paterson, E. Sinn, L.K. Thompson, U. Sakaguchi, Inorg. Chem. 37 (1998) 1028–1036.
[29] A. Hori, M. Yonemura, M. Ohba, H. Okawa, Bull. Chem. Soc. Jpn. 74 (2001) 495–503.
[30] W. Clegg, R.A. Henderson, Inorg. Chem. 41 (2002) 1128–1135.
[31] J. Ruiz, R. Quesada, V. Riera, S.G. Granda, M.R. Diaz, Chem. Commun. 9 (2003) 2028–2029.
[32] P.M. Angus, R.J. Geue, N.K.B. Jensen, F.K. Larsen, C.J. Qin, A.M. Sargeson, J. Chem. Soc., Dalton Trans. 22 (2002) 4260–4263.
[33] C.K. Lai, R. Lin, M.-Y. Lu, K.-C. Kao, J. Chem. Soc., Dalton Trans. 11 (1998) 1857–1862.
[34] B.J. Hathaway, A.A.G. Tomlinson, Coord. Chem. Rev. 5 (1970) 1–6.
[35] T.W. Welch, H.H. Thorp, J. Phys. Chem. 100 (1996) 13829–13836.
[36] J. Liu, T. Zhang, T. Lu, L. Qu, H. Zhou, Q. Zhang, L. Ji, J. Inorg. Biochem. 91 (2002) 269–276.
[37] R.F. Pastenack, E.J. Gibbs, J. Villafranca, J. Biochem. (Tokyo) 22 (1983) 2406–2412.
[38] M. Baidini, M.B. Ferrari, F. Bisceglie, G. Pelosi, S. Pinelli, P. Tarasconi. Inorg. Chem. 42 (2003) 2049–2055; J.K. Barton, A.T. Danishefsky, J.M. Goldberg, J. Am. Chem. Soc. 106 (1984) 2172.
[39] Q. Li, P. Yang, H. Wang, M. Guo, J. Inorg. Biochem. 63 (1996) 79–98.
[40] A. Czarny, D.W. Boykin, A.A. Wood, C.M. Nunn, S. Neidle, M. Zhao, W.D. Wilson, J. Am. Chem. Soc. 117 (1995) 4716–4717.
[41] S. Satyanarayana, J.C. Dabrowiak, J.B. Chaires, Biochemistry 31 (1992) 9319–9324.
[42] S. Satyanarayana, J.C. Dabrowiak, J.B. Chaires, Biochemistry (1993) 2573–2584.

[43] P. Adawadkar, W.D. Wilson, W. Brey, E.J. Gabbay, 97 (1975) 1959–1961, J. Liu, H. Zhang, C. Chen, H. Deng, T. Lu, L. Ji, Dalton Trans (2003) 114–119.

[44] R.S. Srivastava, Inorg. Chim. Acta 56 (1981) 65–67.